Development of chitosan nanocapsules containing essential oil of Matricaria chamomilla L. for the treatment of cutaneous leishmaniasis.

Thaysa Ksiaskiewcz Karam, Sonia Ortega, Tania Ueda Nakamura, Rachel Auzély-Velty, Celso Vataru Nakamura

Development of chitosan nanocapsules containing essential oil of *Matricaria chamomilla* L. for the treatment of cutaneous leishmaniasis

Thaysa Ksiaskiewcz Karam[a], Sonia Ortega[b], Tânia Ueda Nakamura[a], Rachel Auzely-Velty[b*], Celso Vataru Nakamura[a*].

[a] State University of Maringá, Laboratory of Microbiology Applied to Natural and Synthetic Products, Department of Pharmaceutical Sciences, Maringá, Brazil.

[b] University Grenoble Alpes, Centre de Recherche de Macromolecules Végetales, CERMAV – CNRS, Grenoble, France.

* rachel.auzely@cermav.cnrs.fr

* cvnakamura@gmail.com

Abstract

Matricaria chamomilla L. has been used for centuries in many applications, including antiparasitic activity. Leishmaniasis is a parasitic disease, with limited treatments, due to high cost and toxicity. Thus, there is a need to develop new treatments, and in this context, natural products are targets of these researches. We report the development of chitosan nanocapsules containing essential oil of *M. chamomilla* (CEO) from oil-in-water emulsions using chitosan modified with tetradecyl chains as biocompatible shell material. The nanocapsules of CEO (NCEO) were analyzed by optical microscopy and dynamic light scattering, which revealed spherical shape and an average size of 800 nm. Successful encapsulation of CEO was further confirmed by fluorescence microscopy observations taking advantage of the autofluorescence properties of CEO. The encapsulation efficiency was around 90 %. The entrapment of CEO reduced its cytotoxicity towards normal cells. On the other hand, the CEO was active against promastigotes and intracellular amastigotes, exhibiting IC_{50} of 3.33 µg/mL and 14.56 µg/mL, respectively, while NCEO showed IC_{50} for promastigotes of 7.18 µg/mL and for intracellular amastigotes of 14.29 µg/mL. These results demonstrate that encapsulation of CEO in nanocapsules using an alkylated chitosan biosurfactant as a “green” stabilizer is a promising therapeutic strategy to treat leishmaniasis.

Keywords: Nanocapsules; Chitosan; *Matricaria chamomilla*.

1. Introduction

There is a diversity of essential oil (EO) that present biological activities reported in the literature, and among them, the EO of chamomile (CEO), which is extracted from fresh or dried floral chapters of *Matricaria chamomilla* L. [1]. The floral chapters of *M. chamomilla* have between 0.24 - 2% of essential oil [2]. The primary constituents are sesquiterpenes, such as (-)-α-bisabolol (5–70%), bisabolol oxide A (5–60%), bisabolol oxide B (5–60%), bisabolone oxide (0–8%), (E)-β-farnesene (7–45%), chamazulene (1–35%) [3, 4]. Variation of the compounds concentration, as well as variation of the compound in the most abundance, are found in different sample of the CEO. This fact is explained by genetic and technological differences, of which many variables can influence, such as the flowering stage, the flower/stem ratio of the plant material, whether the material is fresh or dry, among others [5].

Many biological activities are attributed to the CEO and some of its major compounds, such as, sedative, antibacterial, antifungal, antispasmodic, antipruritic, anti-inflammatory, antigenotoxic and antioxidant effects [3, 6, 7, 8]. Antiparasitic activity is also reported, especially against the forms of different species of leishmaniasis [9, 10, 11, 12, 13, 14].

Leishmaniasis is a disease caused by protozoa of the genus *Leishmania*, family Trypanosomatidae. There are three forms of this disease, which include cutaneous leishmaniasis, mucocutaneous leishmaniasis and visceral leishmaniasis [15]. According to WHO [16], leishmaniasis is considered to be a neglected disease that causes significant morbidity worldwide. Cutaneous leishmaniasis is the most common form of the disease, with an estimated 1.5 million new cases per year [16]. Available therapeutic approachs against leishmaniasis are scarce, and these treatments (sodium stibogluconate (Pentostam®), *N*-methyl glucamine antimoniate (Glucantime®) Pentamidine and Amphotericin B) have many limitations, such as parenteral administration, long treatment time, high cost, high toxicity, associated with several side effects [17].

In this sense, the search for alternative therapies is an urgent question, and CEO is an attractive option, since its terpenes have lipophilic characteristics, which facilitates penetration into the lipid bilayers of cell membranes. Consequently, these compounds can generate many changes in cellular

structures, including at the mitochondrial level, leading to the death of different pathogens [9, 14].

Although the CEO presents many interesting biological activities, its use as an active compound requires overcoming some challenges, mainly because of its characteristics, such as volatility and susceptibility to degradation reactions at high temperatures, oxygen, pressure and light [18]. In this way, there is a need to reduce problems with stability, to preserve its biological activities, and an interesting alternative is the encapsulation of the CEO [19]. The encapsulation allows transforming the CEO into powder, improving its solubility in physiological media and also, its bioabsorption and effectiveness [20, 21].

Nanocapsules are particularly suited for the encapsulation of CEO because of the droplets small size (few hundreds of nm) as well as, in general, their preparation conditions that do not require high temperature and evaporation steps. However, for the formation of the nanocapsules, there is a need for high concentrations of surfactants, which tends to cause toxicity [22, 23, 24].

Therefore, the search for biodegradable and biocompatible surfactants for stabilizing nanocapsules is increasing, and in this context, a growing attention has been paid to chitosan as a polysaccharide building block to prepare nanocapsules from oil-in-water emulsions [23 25, 26, 27].

Chitosan (CHI) is an attractive natural amino-polysaccharide (a copolymer of D-glucosamine and *N*-acetyl-D-glucosamine) for food and pharmaceutical applications because of its interesting characteristics, such as biocompatibility, low toxicity, biodegradability, and its amino groups which serve as a platform for further reactions [28, 29]. Amphiphilic systems based on chitosan derivatives may be obtained by two different processes: either by chemical modification of the macromolecular backbone, mainly by alkylation through the amino group [30] or by the interaction between the hydrophilic chains and surfactant molecules [31, 32].

In this work, we prepared nanocapsules of CEO using *N*-alkyl chitosan derivatives as polysaccharide-based stabilizing agents and examine the effect of chain length and degree of substitution of the CHI derivatives on the characteristics of the nanocapsules in terms of size and stability. Genipin, a biocompatible natural crosslinker [33, 34] was further used for crosslinking the

chitosan shell and thereby, increasing the stability in physiological media. *In vitro* CEO-release profiles in different pH media were then studied. In addition, the effect of the modified NCEO was evaluated on *L. amazonensis* promastigotes and amastigotes forms, as well as the cytotoxicity in normal cell lines, in comparison with free CEO and nanocapsules containing sunflower oil.

2. Experimental

2.1 Materials

CEO was purchased from Quinarí (Ponta Grossa, PR, Brazil). Dimethyl sulfoxide (DMSO), hexane HPLC grade (> 95%), ethanol (99%), tetrahydrafuran (> 99.9%), folic acid, hemin, Warren's medium, thiazolyl blue tetrazolium bromide (MTT), 1-dodecanal, 1-tetradecanal, $NaCNBH_3$, genipin, mannitol, farnesene, lysozyme from chicken egg white, Tween 80, were purchased from Sigma-Aldrich (France). Acetic acid (100%) and sodium hydroxide (> 99%) were purchased from Merck KGaA (Germany). Brain heart infusion (BHI) was acquired from Beckon Dickinson (Sparks, MD, USA). Fetal bovine serum (FBS), DMEM medium, RPMI 1640 medium, and Giemsa were obtained from Invitrogen (Grand Island, NY, USA). Chitosan Primex (CS, degree of acetylation (DA) = 0.11, weight average molar mass (M_w) = 310 kg/mol, polydispersity (*Đ*) = 1.8) was purchased from Primex EHF (Iceland). The molar mass distribution and the weight-average molar mass of this sample was determined by size exclusion chromatography using a Waters GPC Alliance chromatograph (USA) equipped with a differential refractometer and a light scattering detector (MALLS) from Wyatt (USA); the CHI solution was injected on a TSKgel GMPWxL column (Tosoh Bioscience) at a concentration of 1 mg/mL in 0.2 M acetic acid / 0.15 M ammonium acetate, at a flow rate of 0.5 mL/min and at a column temperature of 30 °C. All of the other reagents were of analytical grade. The water used in all experiments was purified by an Elga Purelab purification system, with a resistivity of 18.2 MΩ cm.

2.2 Synthesis of *N*-alkyl chitosan derivatives

The alkylation of chitosan was performed by a reductive amination reaction as previously described [30] using different aldehydes. The conditions adopted

are the following: chitosan (200 mg) was first dissolved in 0.2 M acetic acid (11 mL) and stirred overnight at room temperature. Ethanol or tetrahydrofuran (THF) was then added to obtain an organic solvent/acetic acid solution ratio of 1/7.3 (v/v). The solvent mixture used for the reaction with 1-dodecanal was the EtOH/acetic acid mixture, whereas it was THF/acetic acid for 1-tetracanal. Then, the aldehyde was added to the chitosan solution under vigorous stirring.

The amount of the aldehydic compound (varying from 10 to 23.33 mg for 1-dodecanal and from 10 to 15 mg for 1-tetradecanal) was adapted to the desired degree of substitution. After addition of the aldehyde, the pH was adjusted to 5-5.1 and $NaCNBH_3$ (630 mg) solubilized in water (6 mL) was then added. After 24 h of reaction at room temperature, the pH was raised to 8 to precipitate the product. The precipitate was washed with several EtOH (or THF)/water mixtures (3/2, 7/3, 4/1 and 9/1, v/v) and finally, dried at room temperature for 48 h. The chemical structure of the different *N*-alkyl CHI derivatives was confirmed by ^1H NMR which also allowed to determine the degree of substitution (DS, average number of alkyl chain per repeating unit). The different *N*-alkyl CHI derivatives synthesized are designated as CHI_xC_y where x reflects the DS (x = 100 DS) and y, the number of carbon atoms of the grafted alkyl chain (Table 1).

Table 1. Degree of substitution of the *N*-alkyl chitosan derivatives, determined by ^1H NMR.

Reference (CHI_xC_y)	Chain	DS
CHI_3C_{12}	1-dodecanal	0.03
CHI_8C_{12}	1-dodecanal	0.08
$CHI_{13}C_{12}$	1-dodecanal	0.13
CHI_4C_{14}	1-Tetradecanal	0.04
CHI_6C_{14}	1-Tetradecanal	0.06

2.3 Viscosity

The viscosity η (Pa.s) in the low shear rate domain of the *N*-alkyl CHI derivatives solubilized in acetate buffer (0.3 M CH_3COOH / 0.05 M CH_3COONa) was determined using a Low Shear 30 viscometer from Contraves at 25 °C.

2.4 Interfacial tension

A drop tensiometer (Tracker, IT Concept, France) was used to measure the interfacial tension *γ* by analyzing the axial symmetric shape (Laplacian profile) of the rising CEO droplet in solutions of initial and *N*-alkyl chitosan (0.17 mg/mL in 0.3 M CH_3COOH/0.05 M CH_3COONa). All the measurements were performed at controlled temperature (25 ± 0.1°C). The chitosan solutions were prepared by stirring in acetate buffer (0.3 M CH_3COOH / 0.05 M CH_3COONa) overnight. All the measurements were made during a sufficiently long time (24 h), in order to follow the effect of ageing on the surface tension.

2.5 Preparation of nanocapsules

In order to optimize the conditions for the synthesis of NCEO, different CEO/CHI_xC_y ratios, concentrations of CHI_xC_y in 0.05 M acetic acid, and CEO volumes in the chitosan solution were used (Table 2). The CHI_xC_y solutions were prepared under constant stirring overnight at room temperature, in pH 5.5.

The NCEO were prepared using 1 mL of CHI_xC_y solution with the appropriate amount of CEO, and the resulting mixture was sonicated for 30 s with 20 % amplitude. After formation of the emulsion, the pH of the NCEO was raised to 12-12.4 by addition of 1 mM aqueous NaOH (12 mL) for neutralization of the charges on amino groups leading to the formation of stable nanocapsules [35]. CHI shell crosslinking was performed by addition of 32 µL of a solution of genipin at a concentration of 0.25 mg/mL in 70% EtOH /water (v/v), under stirring at 400 rpm, at 50 °C for 3 h [36, 37]. Then, the pH of the solution was adjusted to 7.6-7.7, the NCEO was washed twice with hexane, using a separator funnel [38], and the supernatant was reserved for further analysis of the encapsulation efficiency. The NCEO solution was freeze-dried with 0.5% mannitol, for 24 h [39]. The empty nanocapsules (EM) were produced following the same procedure, by replacing the CEO with the sunflower oil.

Table 2. Concentrations of CHI_xC_y and CEO as well as CEO/CHI_xC_y ratios tested for the preparation of NCEO

Ratios $V_{CEO}/[CHI_xC_y]$	**V_{CEO} (µL)**	**$[CHI_xC_y]$ (mg/mL)**
187	15	0.08

340	20.4	0.06
530	37.1	0.07
875	35	0.04

2.6 Evaluation of stability of nanocapsules

The colloidal stability of NCEO produced from the different CHI_xC_y derivatives at pH 12 was evaluated by measuring the mean diameter using a Zetasizer NanoZS Malvern Instruments apparatus operating with a HeNe laser at 173°. Dilutions of NCEO were prepared in ultrapure water (1:20). Evaluation occurred in the 1st, 15th and 30th days after obtaining the nanocapsules. The stability of nanocapsules at pH 7.4-7.6 was also evaluated by light and fluorescence microscopy using a Zeiss Axioskop 2 microscope equipped with a camera. Analyses were performed in triplicate and expressed as the mean ± standard deviation.

2.7 Characterization of NCEO prepared from CHI_4C_{14}

2.7.1 Mean diameter and polydispersity index

The mean diameter and the polydispersity index were determined by dynamic light scattering (DLS), using a Zetasizer NanoZS Malvern Instruments apparatus operating with a HeNe laser at 173°. Dilutions of NCEO and EM were prepared in ultrapure water (1:20). The analyses were performed in triplicate. The values of mean diameter and polydispersity index were expressed as mean ± standard deviation of the representatives samples, with n=10.

2.7.2 Images in light and fluorescence microscopy

The morphology of the NCEO was analyzed by light and fluorescence microscopy using a Zeiss Axioskop 2 microscope equipped with a camera. For that, the NCEO were prepared in ultrapure water and analyzed. These analyses were performed in triplicate.

2.7.3 Encapsulation efficiency (EE %)

The first step for the determination of the encapsulation efficiency (EE) of the CEO relied on the identification of the main compounds of the CEO. These

analyses were performed using a Focus GC gas chromatograph (Thermo-Finnigan) coupled to DSQ II mass spectrometer (Thermo-Finnigan), equipped with a fused silica capillary DB-5 column (L: 30 mm x I.D.: 0.25 mm, Ft.: 0.25 µm) containing 5% phenyl and 95% methylpolysiloxane (J & W Scientific). The temperature program was as follows: from 40 to 270°C for 2°C/min until 170°C, after which, rate of increase was 50°C/min until 270°C; helium was used as a carrier at a flow rate of 1 mL/min; 1 µL of oil injection; 270°C transfer line temperature; 270°C ion source temperature; 1:10 splitting ratio; 70 eV ionization energy; 50-400 amu scan range; 0.72 s scan time. Data acquisition was carried out using the Xcalibur software. The identification of the main compounds of the CEO was based on the comparison of the retention indices (RI) with the RI values previously published [40] and in the NIST MS Search 2.0 library. The relative percentage of CEO constituents was determined from the peak areas.

The CEO content in chitosan nanocapsules was determined based on the peak of the major compound of the CEO, farnesene, using the same equipment previously described, with modifications of the following parameters: temperature programming conditions were 80-270 ºC at 20 °C/min until 120° and after 2 °C/min until 150 °C, and 50 °C/min until 270 °C. Helium at 1 mL/min was used as a carrier gas; 1 µL of injection; 250 ºC transfer line temperature; 270 ºC ion source temperature; 1:10 splitting ratio; 70 eV ionization energy; 50- 400 amu scan range; 0.72 s scan time. Data acquisition and peak integration were performed using the Xcalibur Xcalibur software.

The farnesene peak present in the CEO was compared to that of commercial farnesene for confirmation of its identification. This analysis allowed establishing a calibration curve for the CEO, using the peak corresponding to farnesene. This curve was then used for the determination of the EE of NCEO based on farnesene, from the amount of non-encapsulated CEO extracted with hexane. The result of the EE% was expressed by mean ± standard deviation of representatives samples, with n=10.

2.7.4 *In vitro* release studies

NCEO were submitted to *in vitro* release studies by the shaking method [41]. In the first release studies, samples of NCEO containing 1 mg of CEO were

diluted in 10 mL of 10 mM PBS buffer, containing 0.5% Tween 80 [42, 43, 44], at pH 5.5 and 7.4. The NCEO dispersions in PBS buffer were incubated on an orbital stirrer at 37 °C under constant stirring at 150 rpm. At predetermined times (0.15, 0.30, 1, 2, 4, 6, 12, 24, 48 and 72 h), the NCEO were washed twice with hexane, using a separatory funnel, and the supernatant was reserved and analyzed by GC. The cumulative percentage of CEO released was plotted against time. Analyses were performed in triplicate and expressed as the mean ± standard deviation.

2.8 *In vitro* biological assays

2.8.1 Parasites and Cell Culture

L. amazonensis strain WHOM/BR/75/Josefa was originally isolated from a human case of diffuse cutaneous leishmaniasis by C. A. Cuba at University of Brasília, DF, Brazil). Promastigote forms were cultured in Warren's medium supplemented with 10% heat-inactivated FBS at 25°C. J774A1 macrophages were maintained in RPMI 1640 medium with sodium bicarbonate and L-glutamine (pH 7.2), supplemented with 10% FBS at 37 °C in a 5% CO_2. HaCat immortalized human keratinocyte cells (CLS Cell Lines Service 300493) and Vero (CCL-81) were grown in Dulbeccos Modified Eagle Medium (DMEM) without glutamine, added with pyruvate and supplemented with 10% fetal bovine serum, kept at 37 °C with 5% of CO_2.

2.8.2 Cytotoxicity assay

The cytotoxicity was evaluated against the following cell lines: HaCat (CLS Cell Lines Service, 300493), J774A1 macrophages and Vero (CCL-81) using the MTT reduction cell viability assay [45].

The cells lines (HaCat / Macrophages / Vero) were cultured in 96-well microplates at a concentration of 5 x 10^5 cells/mL, in appropriate medium for each cell type supplemented with 10% fetal bovine serum, maintained at 37° C and 5% of CO_2 for 24 h. After this time, the NCEO, EM and free CEO and sunflower oil were added in increasing concentrations (0.1 – 1000 µg/mL), and the microplate was then incubated for 48 h. After treatment, cells were incubated in the presence of MTT (2 mg / mL) for 4 h. After, the supernatant was removed and was added

DMSO, with the complete solubilization of the formazan crystals the absorbance reading was carried out at 570 nm in a microplate spectrophotometer (Power Wave XS - Bio-Tek). The concentration that inhibited the absorbance by 50% compared to the untreated control (CC_{50}) was determined. Data were obtained from at least three independent experiments and were expressed as means ± standard deviation.

2.8.3 Antiproliferative assay

The promastigote forms of *L. amazonensis* with 48 h of culture were incubated at a concentration of 1×10^6 cells/mL in culture medium supplemented with 10% fetal bovine serum in 96-well plates with different concentrations (0.1 - 1000 µg/mL) of NCEO, EM and free CEO and sunflower oil, to evaluate the survival rate of the parasite. The plates were incubated for 72 h at 25 ° C. After the incubation, the contents of each well were diluted in 3% formalin and counted on a Neubauer hemocytometer, and the IC_{50} values were determined by the percentage of inhibition of 50% of the parasites compared with the untreated promastigote control. The data are showed as mean ± standard deviation, from at least three independent experiments.

2.8.4 Interaction between *L. amazonensis* and culture macrophages

J774A1 macrophages (5×10^5 cells/ml) and promastigotes (5×10^6 parasites/mL) in RPMI 1640 medium supplemented with 10% FBS were dispensed into round glass coverslips in 24 well plates for 24 h in stove supplemented with CO_2 (5%) at 36 ºC to promote interaction between macrophages and parasites. After this period the culture medium was removed by aspiration to remove the non-adhered cells to the coverslips and then the cells were treated with different concentrations of NCEO, EM and free CEO and sunflower oil, and incubated under the same conditions for 48 h. After the incubation time the cells were fixed with 0.1 M sodium cacodylate buffer and 2.5% glutaraldehyde buffer for 72 h. Thereafter, the coverslips were stained with 5% Giemsa solution and mounted on glass slide with Permount. The count of about 200 cells was performed under an optical microscope and the established

survival rate (multiplying the percentage of macrophages infected by the average number of parasites by macrophages), and IC_{50} were determined. At least three independent experiments have been carried out, and the results are expressed as means ± standard deviation.

3. Results and discussion

3.1 Synthesis and characterization of the *N*-alkyl chitosan derivatives and preparation of nanocapsules

The *N*-alkyl chitosan derivatives were prepared by reductive amination reactions carried out in homogeneous conditions using 1-dodecanal or 1-tetradecanal, as previously described [30]. As these alkylating conditions are non-destructive for the polymer [30], the *N*-alkyl (dodecyl (C_{12}) or tetradecyl (C_{14})) chitosan samples possess the same degree of polymerization as initial chitosan. Several dodecyl and tetradecyl chitosan derivatives with degrees of substitution ranging from 0.03 to 0.15, derived from ^{1}H NMR spectroscopy analysis (Figure S1), were synthesized by varying the monomolar ratio chitosan/aldehyde.

These amphiphilic polymers are known to have associating properties even in diluted aqueous solutions. Therefore, we investigated the role of the alkyl chain length and density of grafting on the viscosity of solutions of initial CHI and the *N*-alkyl chitosan derivatives (CHI_xC_y) in the low concentration regime and at low shear rates. The experimental data obtained from solutions at 0.5 and 1 g/L are given in Figure 1. As can be seen from this figure, the solutions of the two *N*-tetradecyl CHI derivatives (CHI_4C_{14} and CHI_6C_{14}) and of the *N*-dodecyl CHI derivative with the lowest DS (CHI_3C_{12}) exhibit higher viscosities than those of the *N*-dodecyl CHI derivatives with higher DS (CHI_8C_{12} and $CHI_{13}C_{12}$) and initial chitosan. The large increase of viscosity observed for CHI_4C_{14}, CHI_6C_{14}, CHI_3C_{12} can be attributed to hydrophobic interactions between the grafted alkyl chains. These hydrophobic domains play the role of junction points between the chitosan chains, resulting in loosely crosslinked networks. On the other hand, when the amount of grafted alkyl chain becomes high, as in the case of the CHI_8C_{12} and $CHI_{13}C_{12}$ derivatives, it can be assumed that the hydrophobic interactions favor more self-aggregation of the chitosan derivatives. This is supported by the fact

that the viscosities measured for the solutions of CHI_8C_{12} and $CHI_{13}C_{12}$ are lower than those of initial chitosan.

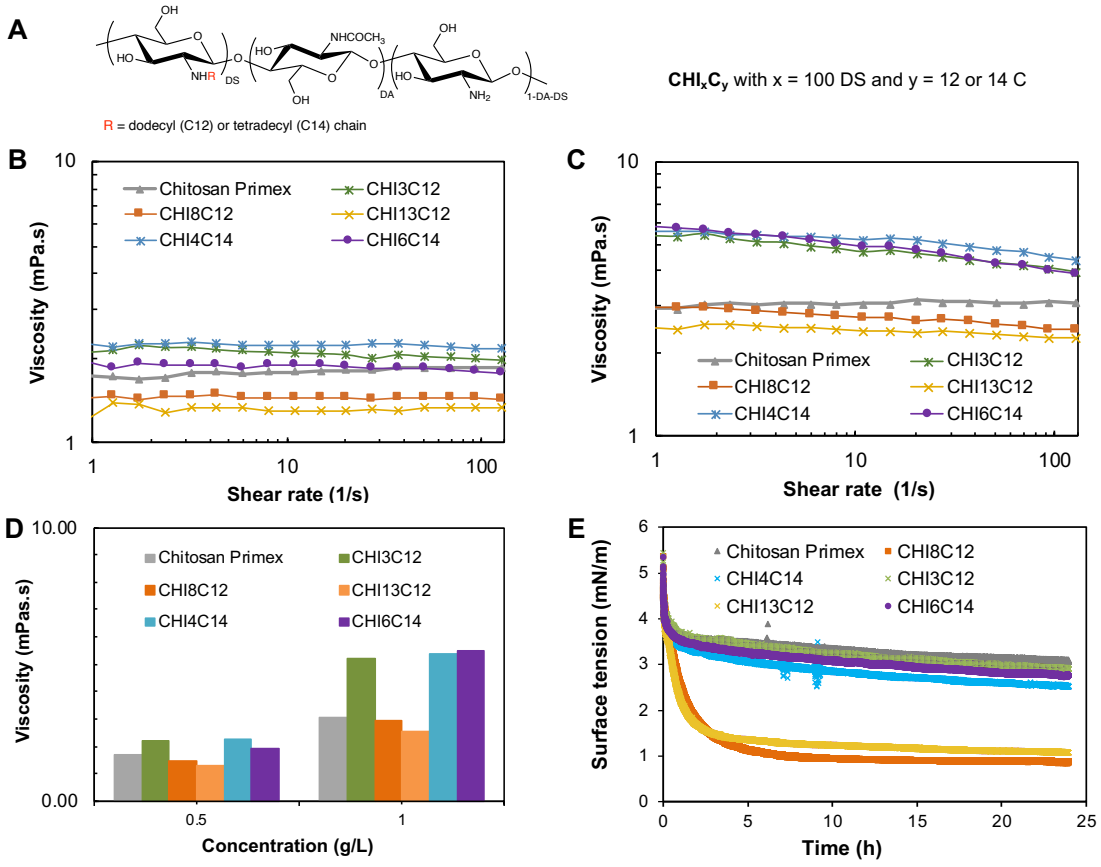

Figure 1. Viscosity of solutions of *N*-alkyl chitosan derivatives and initial chitosan, and interfacial tension evolution measured from CEO droplets in solutions of *N*-alkyl chitosan derivatives and initial chitosan at 25 °C. Solvent of the chitosan solutions: 0.3 M CH_3COOH / 0.05 M CH_3COONa. A) Chemical structure of the *N*-alkyl chitosan derivatives. B) and C) Viscosity as a function of shear rate at polymer concentrations of 0.5 and 1 g/L, respectively. D) Viscosity at low shear rate (Newtonian plateau) as a function of polymer concentration for different alkyl chain lengths and DS. E) Interfacial tension evolution of CEO droplets in chitosan solutions.

The analysis of the interfacial tension (γ) of a droplet of CEO suspended in solutions of the different chitosan samples also revealed a different behavior for the CHI_8C_{12} and $CHI_{13}C_{12}$ derivatives (Figure 1E). From Figure 1E, it can be observed that γ drops with time for initial CHI and all the CHI_xC_y derivatives, indicating progressive diffusion of the polymers toward the interface and

stabilization. However, the decrease of γ occurs more rapidly and more significantly for the CHI_8C_{12} and $CHI_{13}C_{12}$ derivatives.

All these derivatives as well as initial chitosan were then investigated for the formation of NCEO. The procedure used for the synthesis of NCEO is illustrated in Figure 2. The first step consisted in the formation of oil-in-water nanocapsules at pH 5.5, by sonication of the CHI_xC_y/CEO mixtures. Aqueous NaOH was then added to neutralize the charges of CHI_xC_y and thereby, increase the hydrophobicity and emulsion-stabilizing property of the chitosan derivatives [35].

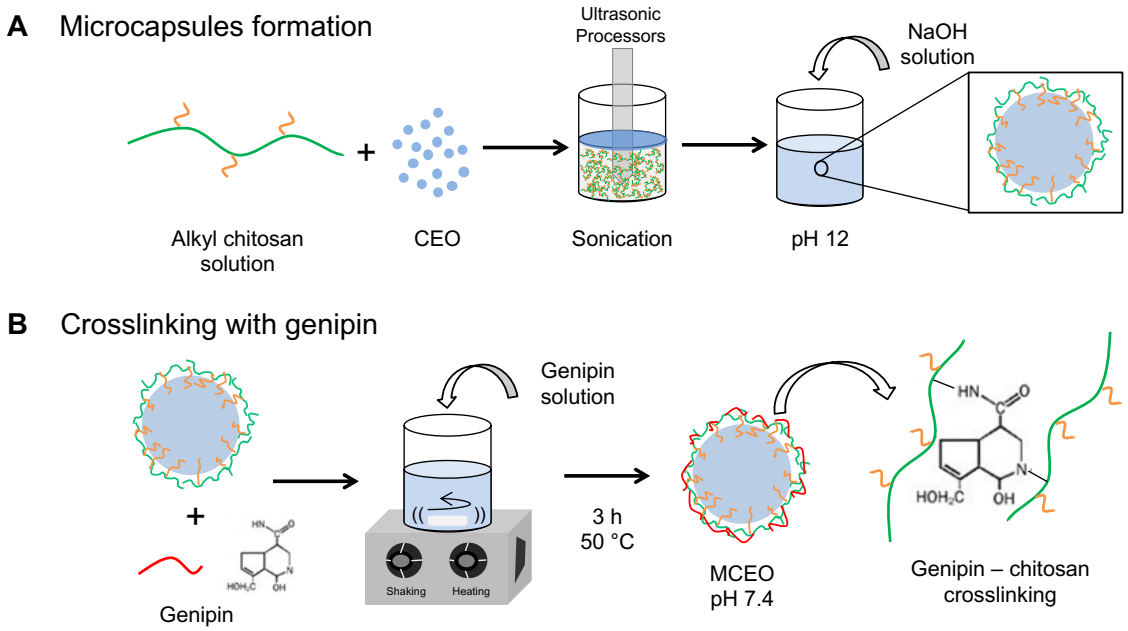

Figure 2. Schematic representation of the procedure for the preparation of NCEO.

In the second step, the chitosan shell was crosslinked with genipin in order to ensure better stabilization and strengthen the shell structure at physiological pH. Genipin reacts with compounds containing primary amine groups, such as chitosan, to form covalently crosslinked networks [33, 46]. This natural cross-linker is about 5000–10000 times less cytotoxic than glutaraldehyde [47, 48].

The nanocapsules formed using different ratios of CEO/CHI_xC_y were investigated for their stability at pH 12 for 30 days. The analyses were conducted

by DLS in order to determine the mean diameter of the NCEO. The results obtained are displayed in Figure 3. As can be seen from this figure, the NCEO produced from CHI_8C_{12} and $CHI_{13}C_{12}$ show greater variations among the tested ratios, ranging from 700 to 1800 nm. The self-aggregation behavior of these derivatives observed from the viscosity measurements probably the reason for this result. Moreover, the nanocapsules prepared from the *N*-dodecyl chitosan samples were the less stable over time, showing larger variations in the mean diameters. Regarding the NCEO prepared from the *N*-tetradecyl CHI samples, that obtained from CHI_4C_{14}, with the ratio of 187, exhibited the lowest variation in mean diameters as a function of time. It is interesting to note that this derivative led to the largest increase of viscosity in dilute conditions but moderate decrease of the CEO-water interfacial tension. This point out the importance of precisely controlling the hydrophilic/lipophilic balance of the amphiphilic CHI derivative to make it suitable for stabilization of the oil-water interface.

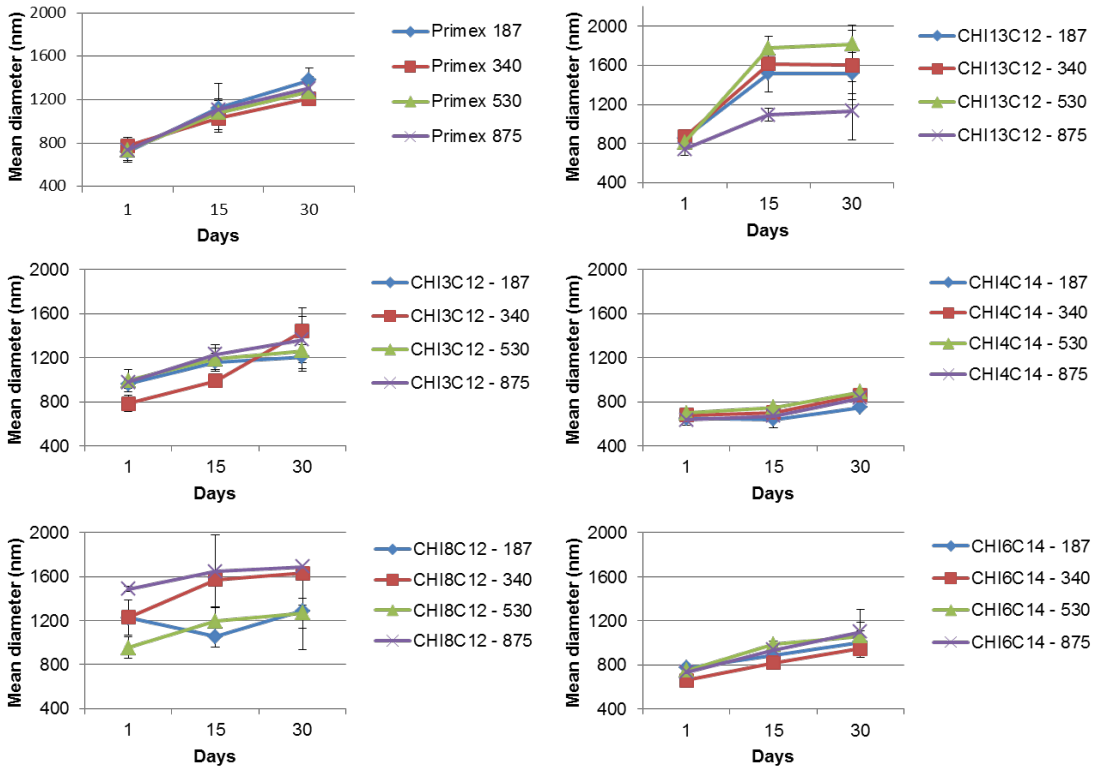

Figure 3. Stability of the NCEO obtained from different modified chitosan at pH 12, by DLS. Relationship of the mean diameter x time.

After adjusting the pH of the nanocapsule solution to 7.4, the NCEO were observed by optical and fluorescence microscopy, in order to assess their stability. It was possible to evaluate the behavior of NCEO by means of fluorescence microscopy due to the autofluorescence properties of the CEO.

The NCEO produced with chitosan Primex (Figure 4A), that is the chitosan without modification, as well as NCEO produced from the N-dodecyl chitosan samples (Figures 4B, 4C and 4D) were unstable in pH 7.4, and it was possible to observe that this instability resulted in release of oil from the nanocapsules. The NCEO produced from CHI_6C_{14} did not show much release of the CEO (Figures 4F); however, significant aggregation of the NCEO occurred. Thus, only the NCEO prepared with the CH_4C_{14} remained stable, without aggregates and without releasing the CEO, both at basic and neutral pH (Figures 4E).

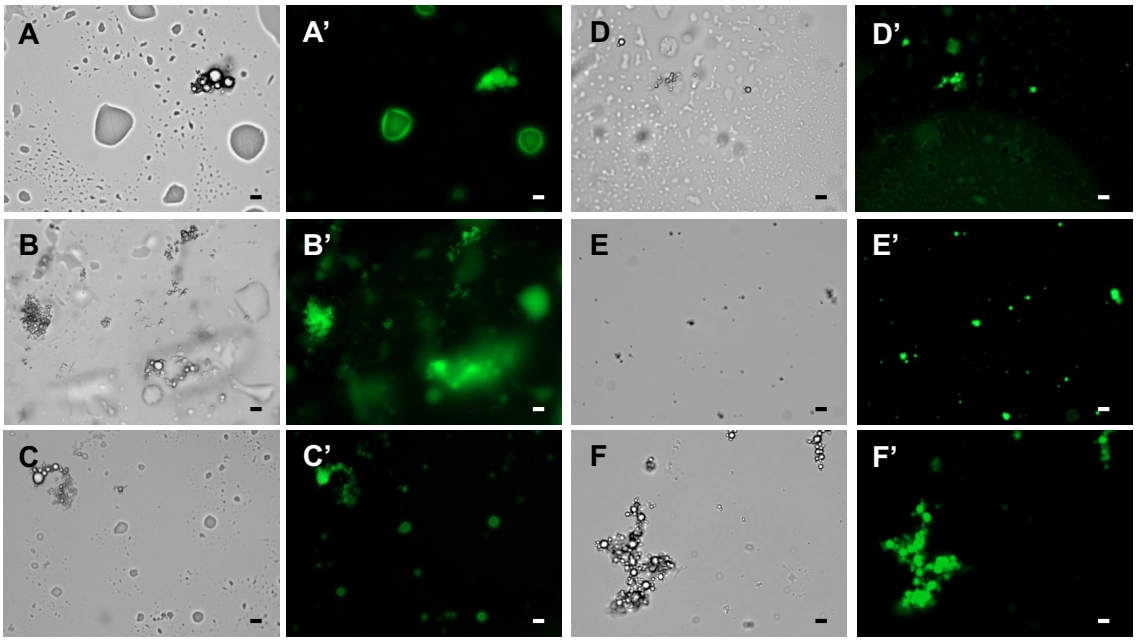

Figure 4. Stability of the NCEO obtained from different modified chitosan (187 ratios) in pH 7.4, by optical and fluorescence microscopy (400x). NCEO prepared with CHI Primex (A and A'); CHI_3C_{12} (B and B'); CHI_8C_{12} (C and C'); $CHI_{13}C_{12}$ (D AND D'), CHI_4C_{14} (E and E') and CHI_6C_{14} (F and F'). All bars = 5 µm.

Based on these results, the NCEO prepared from CHI_4C_{14} was selected for the biological tests.

3.2 Physicochemical characterization of NCEO prepared from CHI_4C_{14}

Dynamic light scattering performed at 25 °C revealed a similar size for the NCEO and the nanocapsules containing sunflower oil (average diameter of 801 and 828 nm, respectively, Table 3). The spherical shape of the nanocapsules containing CEO was confirmed by optical and fluorescence microscopy (Figure 5).

Table 3. Average diameter and polydispersity index of the NCEO and EM in ultrapure water at 25 °C.

	Avarege diameter (nm)	**PdI**
NCEO	801.33 ± 14.74	0.310 ± 0.01
EM	827.77 ± 17.08	0.385 ± 0.04

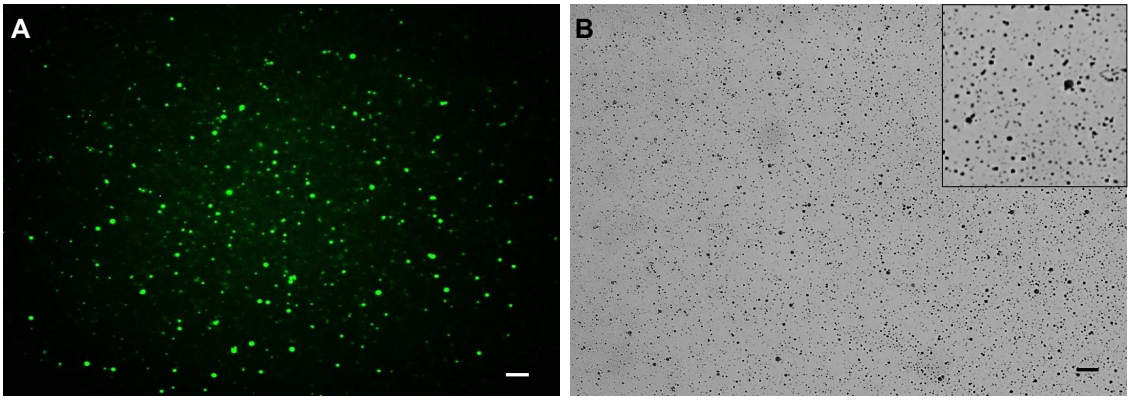

Figure 5. Fluorescence and phase contrast images of NCEO in ultrapure water. A) Fluorescence image (400x) and B) Phase contrast image (400x). All bars = 10 μm.

The EE was determined based on the most abundant compound of the CEO. For this, the main components of the CEO were identified and quantified by GC-MS. This analysis revealed that the most abundant constituent of CEO is the (Z)-β-farnesene (39.87%), followed by α-bisabolol oxide B (13.05%), α-bisabolol oxide A (10.4%), (E,E)-α-farnesene (6.47%) and α-bisabolol (5.74%); these results corroborated with data shown in other studies [5, 49].

Then, after the identification and confirmation of the major compound of the CEO, the amount of non-encapsulated farnesene was quantified, allowing to determine the EE based on farnesene. The EE was estimated at 89.9 ± 2.5 %.

3.2.1 *In vitro* release of the CEO

The release profiles of the CEO from the nanocapsules were investigated *in vitro* at ambient temperature for 3 days. The media used were phosphate buffer saline containing Tween 80 at two different pH (physiological pH and a pH closed to the pH of skin (5.5). The % cumulative release was less than 10 % at both pH within this period (Figure 6).

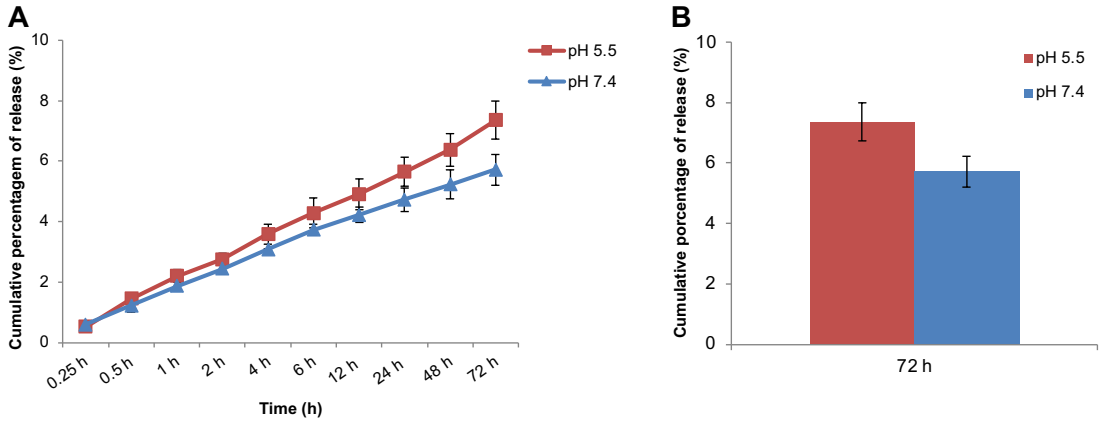

Figure 6. A) Percentage cumulative release of CEO from NCEO in phosphate buffer saline with 0.5% (v/v) tween 80, at pH 5.5 and pH 7.4, at predetermined times. B) Cumulative percentage of CEO at pH 5.5 and pH 7.4. The release at pH 5.5 is statistically different from pH 7.4. Statistical analyzes were performed with ANOVA one way - multiple comparisons, $p < 0.05$.

3.2.2 *In vitro* biological assays

The cytotoxicity of NCEO was investigated in keratinocyte cells, macrophages and Vero cells by MTT assay after 48h of incubation and compared to that of the nanocapsules containing the sunflower oil (EM). The results summarized in Table 4 show that encapsulation of the CEO reduces its cytotoxicity towards the three mammalian cells. Regarding the EM and free sunflower oil, they did not present toxicity in the concentrations used.

Table 4. Cytotoxic evaluation of NCEO, EM and free CEO against the cell lines HaCat, macrophages and Vero.

	HaCat	**Macrophages**	**Vero**
	CC_{50} (µg/mL)	**CC_{50} (µg/mL)**	**CC_{50} (µg/mL)**
Free CEO	70 ± 2	19.71 ± 1.73	181.73 ± 7.88

NCEO	167.86 ± 9.45	207.92 ± 18.53	608.3 ± 25.69
EM	> 1000	> 1000	> 1000
Sunflower oil	> 1000	> 1000	> 1000

The antiproliferative activity of the NCEO against the *L. amazonensis* promastigotes and amastigotes forms was estimated by direct counting. The CC_{50} values shown in Table 5 indicate that the encapsulated CEO maintains a very interesting activity against both forms of *L. amazonensis*.

From Figure 7, significant differences in the amount of intracellular amastigotes, between the control (untreated) (A) and macrophages treated with the free CEO (B) and NCEO (C) can be obtained. In both forms of *L. amazonensis*, the EM and free sunflower oil did not present activity.

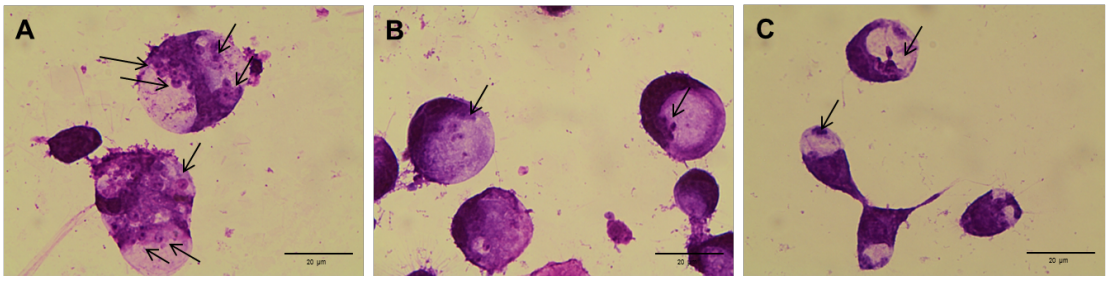

Figure 7. Optical microscopy of macrophages infected with intracellular amastigotes (black arrows) of *L. amazonensis* (A-C) (400x). (A) Infected macrophages without treatment (control group); (B) Infected macrophages treated with IC_{50} of free CEO (14.56 µg/mL) and (C) Infected macrophages treated with IC_{50} of NCEO (14.29 µg/mL). Scale bars: 20 µm (A-C).

Table 5. Activity evaluation of NCEO, EM and free CEO against promastigotes and amastigotes of *L. amazonensis.*

	Promastigotes IC_{50} (µg/mL)	**Amastigotes IC_{50} (µg/mL)**
Free CEO	3.33 ± 0.38	14.56 ± 2.34
NCEO	7.18 ± 0.7	14.29 ± 1.01
EM	> 1000	> 1000
Sunflower oil	> 1000	> 1000

Another interesting result is the selectivity index obtained for the NCEO. The selectivity index (SI = CC_{50}/IC_{50}) is a value that relates the activity with the

cytotoxicity. The higher the selectivity index, the more selective the drug is for protozoa. Table 6 shows the selectivity index with respect to the macrophages cells. Very interestingly, the value of the selectivity index increased when the CEO is encapsulated in the nanocapsules, passing from 1.35 to 14.55 for the amastigote forms.

Table 6. Selectivity index (SI) of intracellular amastigotes of *L. amazonensis* with respect to macrophages cells.

	SI
	Amastigotes
Free CEO	1.35
NCEO	14.55

The *in vitro* activity of the CEO and the NCEO against intracellular amastigotes were very similar, and this can be explained by the macrophage ability to uptake the nanoparticles, a fact that has already been demonstrated in other studies with chitosan nanoparticles [50, 51]. In our release assay, only the pH variable was evaluated, in which NCEO released a small percentage of CEO, however, in the *in vitro* assay against macrophages infected with amastigotes, after the internalization of NCEO, the nanoparticles were exposed to the macrophage intracellular content, which probably led to the release of the CEO. This may explain the activity similar to the CEO.

4. Conclusion

In this study, nanocapsules containing essential oil of *M. chamomilla* were produced from a chitosan derivative modified with *N*-tetradecyl chains. The nanocapsules were prepared by oil-in-water emulsion using the amphiphilic chitosan as a green surfactant to stabilize droplets of essential oil of *M. chamomilla* followed by crosslinking the shell with genipin. These crosslinks provided physiological stability and the maintenance of the essential oil within the nanocapsules. *In vitro* biological studies showed that the essential oil of *M. chamomilla* into nanocapsules maintained the activity against the forms of *L. amazonensis*. On the other hand, the nanocapsules containing the essential oil

of *M. chamomilla* showed a significant reduction in cytotoxicity against mammalian cells, in comparison with the free essential oil. These results suggest that these nanocapsules hold great potential in anti-leishmanial therapy, due to their physicochemical characteristics combined with their biological activity maintenance and reduction of cytotoxic effects.

Acknowledgements

The authors are grateful to the "Conselho Nacional de Desenvolvimento Científico e Tecnológico (CNPq) for financial support (grant no. 401286/2014-2 PVE)". T. K. K. gratefully acknowledges the "Science without Borders Program" of CNPq for the sandwich doctorate scholarship. This work was also supported by the "Capacitação de Aperfeiçoamento de Pessoal de Nível Superior (CAPES)", "PRONEX/Fundação Araucária (Paraná-Brazil)"; "Financiadora de Estudos e Projetos (FINEP-Brazil)"; "Programa de Pós-Graduação em Ciências Farmacêuticas da Universidade Estadual de Maringá"; "Complexo de Centrais de Apoio a Pesquisa (COMCAP-UEM)"; and the CAPES-COFECUB program (Ph-C 911/18).

References

[1] V. Gupta, P. Mittal, P. Bansal, S. L. Khokra, D. Kaushik, Pharmacological potential of *Matricaria recutita*-A review, Int J. Pharm. Sci. Drug Res. 2 (2010) 12-6. http://ijpsdr.com/index.php/ijpsdr/article/view/68

[2] N. Tsivelika, E. Sarrou, K. Gusheva, C. Pankou, T. Koutsos, P. Chatzopoulou, A. Mavromatis, Phenotypic variation of wild Chamomile (*Matricaria chamomilla* L.) populations and their evaluation for medicinally important essential oil, Biochem. Syst. Ecol., 80 (2018) 21-28. https://doi.org/10.1016/j.bse.2018.06.001

[3] L. P. Stanojevic, Z. R. Marjanovic-Balaban, V. D. Kalaba, J. S. Stanojevic, D. J. Cvetkovic, Chemical composition, antioxidant and antimicrobial activity of chamomile flowers essential oil (*Matricaria chamomilla* L.), J. Essent. Oil Bear. Pl. 19 (2016) 2017-2028. https://doi.org/10.1080/0972060X.2016.1224689

[4] M. Sharifi-Rad, J. Nazaruk, L. Polito, M. F. B. Morais-Braga, J. E. Rocha, H. D. M. Coutinho, B. Salehie, G. T. C. Montanari, M. M. Contreras, Z. Yousaf, W. N. Setzer, D. R. Verma, M. Martorell, A. Sureda, J. Sharifi-Rad. *Matricaria genus* as a source of antimicrobial agents: From farm to pharmacy and food applications, Microbiol. Res. 215 (2018) 76-88. https://doi.org/10.1016/j.micres.2018.06.010

[5] L. P. Stanojevic, Z. R. Marjanovic-Balaban, V. D. Kalaba, J. S. Stanojevic, D. J. Cvetkovic. Chemical Composition, Antioxidant and Antimicrobial Activity of Chamomile Flowers Essential Oil (*Matricaria chamomilla* L.), J Essent Oil Bear Pl. 19 (2016), 2017 – 2028. https://doi.org/10.1080/0972060X.2016.1224689

[6] O. Singh, Z. Khanam, N. Misra, M. K. Srivastava. Chamomile (*Matricaria chamomilla* L.): an overview, Pharmacogn. Rev. 5 (2011) 82. 10.4103/0973-7847.79103

[7] Ö. D. Can, Ü. D. Özkay, H. T. Kıyan, B. Demirci. Psychopharmacological profile of Chamomile (*Matricaria recutita* L.) essential oil in mice, Phytomedicine 19 (2012) 306-310. https://doi.org/10.1016/j.phymed.2011.10.001

[8] M. C. Romero, A. Valero, J. Martín-Sánchez, M. C. Navarro-Moll. Activity of *Matricaria chamomilla* essential oil against anisakiasis, Phytomedicine 19 (2012) 520-523. https://doi.org/10.1016/j.phymed.2012.02.005

[9] M. Morales-Yuste, F. Morillas-Marquez, J. Martin-Sanchez, A. Valero-López, M. C. Navarro-Moll. Activity of (−) alpha-bisabolol against *Leishmania infantum* promastigotes, Phytomedicine. 17 (2010) 279–281. https://doi.org/10.1016/j.phymed.2009.05.019

[10] A. Gawde, C. L. Cantrell, V. D. Zheljazkov, T. Astatkie, V. Schlegel. Steam distillation extraction kinetics regression models to predict essential oil yield, composition, and bioactivity of chamomile oil, Ind. Crop. Prod. 58 (2014) 61-67. https://doi.org/10.1016/j.indcrop.2014.04.001

[11] M. M. Rottini, A. C. F. Amaral, J. L. P. Ferreira, J. R. de Andrade Silva, N. N. Taniwaki, C. D. S. F. de Souza, L. N. Escoffier, F. Almeida-Souza, D. J. Hardoim, S. C. G. da Costa, K. da Silva Calabrese. *In vitro* evaluation of (−) α-bisabolol as a promising agent against *Leishmania amazonensis*. Exp. Parasitol. 148 (2015) 66-72. https://doi.org/10.1016/j.exppara.2014.10.001

[12] M. A. Andrade, C. dos Santos Azevedo, F. N. Motta, M. L. dos Santos, C. L. Silva, J. M. de Santana, I. M. Bastos. Essential oils: in vitro activity against *Leishmania amazonensis*, cytotoxicity and chemical composition, BMC Complem. Altern. M. 16 (2016) 444. https://doi.org/10.1186/s12906-016-1401-9

[13] V. Corpas-López, G. Merino-Espinosa, V. Díaz-Sáez, F. Morillas-Márquez, M. C. Navarro-Moll, J. Martín-Sánchez. The sesquiterpene (−)-α-bisabolol is active against the causative agents of Old World cutaneous leishmaniasis through the induction of mitochondrial-dependent apoptosis, Apoptosis. 21 (2016) 1071-1081. https://doi.org/10.1007/s10495-016-1282-x

[14] S. Hajaji, I. Sifaoui, A. López-Arencibia, M. Reyes-Batlle, I. A. Jiménez, I. L. Bazzocchi, B. Valladares, H. Akkari, J. Lorenzo-Morales, J. E. Piñero. Leishmanicidal activity of α-bisabolol from *Tunisian chamomile* essential oil,

Parasitol. Res. 117 (2018) 2855-2867. https://doi.org/10.1007/s00436-018-5975-7

[15] S. Burza, S. L. Croft, M. Boelaert. Leishmaniasis, The Lancet, 393 (2018) 872-873. https://doi.org/10.1016/S0140-6736(18)31204-2

[16] WHO. World Health Organization. (2011). Working to overcome the global impact of neglected tropical diseases—Summary: Introduction. Weekly Epidemiological Record= Relevé épidémiologique hebdomadaire, 86(13), 113-120. https://apps.who.int/iris/handle/10665/241731

[17] N. E. Aronson, C. A. Joya. Cutaneous Leishmaniasis: Updates in Diagnosis and Management, Infect. Dis. Clin. 33 (2019) 101-117. https://doi.org/10.1016/j.idc.2018.10.004

[18] A. Mohammadi, M. Hashemi, S. M. Hosseini. Chitosan nanoparticles loaded with *Cinnamomum zeylanicum* essential oil enhance the shelf life of cucumber during cold storage. Postharvest Biol. Tec. 110 (2015) 203-213. https://doi.org/10.1016/j.postharvbio.2015.08.019

[19] S. Chatterjee, Z. M. Judeh. Encapsulation of fish oil with N-stearoyl O-butylglyceryl chitosan using membrane and ultrasonic emulsification processes, Carbohyd. Polym. 123 (2015) 432-442. https://doi.org/10.1016/j.carbpol.2015.01.072

[20] A. Esmaeili, A. Asgari. In vitro release and biological activities of Carum copticum essential oil (CEO) loaded chitosan nanoparticles. Int. J. Biol. Macromol. 81 (2015) 283-290. https://doi.org/10.1016/j.ijbiomac.2015.08.010

[21] S. P. De Matos, H. F. Teixeira, Á. A. de Lima, V. F. Veiga-Junior, L. S. Koester. Essential Oils and Isolated Terpenes in Nanosystems Designed for Topical Administration: A Review, Biomolecules. 9 (2019) 138. https://doi.org/10.3390/biom9040138

[22] A. El Asbahani, K. Miladi, W. Badri, M. Sala, E. A. Addi, H. Casabianca, A. El Mousadike, D. Hartmanna, A. Jilale, F. N. R. Renaud, A. Elaissari. Essential oils: from extraction to encapsulation, Int. J. Pharmaceut. 483 (2015) 220-243. https://doi.org/10.1016/j.ijpharm.2014.12.069

[23] N. Hasheminejad, F. Khodaiyan, M. Safari. Improving the antifungal activity of clove essential oil encapsulated by chitosan nanoparticles, Food Chem. 275 (2019) 113-122. https://doi.org/10.1016/j.foodchem.2018.09.085

[24] C. Maupas, B. Moulari, A. Béduneau, A. Lamprecht, Y. Pellequer. Surfactant dependent toxicity of lipid nanocapsules in HaCaT cells, Int. J. Pharm. 411 (2011), 136 - 141. https://doi.org/10.1016/j.ijpharm.2011.03.056

[25] S. F. Hosseini, M. Zandi, M. Rezaei, F. Farahmandghavi. Two-step method for encapsulation of oregano essential oil in chitosan nanoparticles: Preparation,

characterization and in vitro release study, Carbohyd. Poly. 95 (2013) 50-56. http://dx.doi.org/10.1016/j.carbpol.2013.02.031

[26] M. Hadidi, S. Pouramin, F. Adinepour, S. Haghani, S. M. Jafari. Chitosan nanoparticles loaded with clove essential oil: Characterization, antioxidant and antibacterial activities, Carbohyd. Poly. 236 (2020), 116075. https://doi.org/10.1016/j.carbpol.2020.116075

[27] A.K. López-Meneses, M. Plascencia-Jatomea, J. Lizardi-Mendoza, D. Fernández-Quiroz, F. Rodríguez-Félix, R.R. Mouriño-Pérez, M.O. Cortez-Rocha. Schinus molle L. essential oil-loaded chitosan nanoparticles: Preparation, characterization, antifungal and anti-aflatoxigenic properties. LWT-Food Sci Technol. 96 (2018), 597 – 603. https://doi.org/10.1016/j.lwt.2018.06.013

[28] Q. Ma, Y. Zhang, F. Critzer, P. M. Davidson, S. Zivanovic, Q. Zhong. Physical, mechanical, and antimicrobial properties of chitosan films with microemulsions of cinnamon bark oil and soybean oil, Food Hydrocol. 52 (2016) 533-542. https://doi.org/10.1016/j.foodhyd.2015.07.036

[29] Y. Shao, C. Wu, T. Wu, Y. Li, S. Chen, C. Yuan, Y. Hu. Eugenol-chitosan nanoemulsions by ultrasound-mediated emulsification: Formulation, characterization and antimicrobial activity, Carbohyd. Polym. 193 (2018) 144-152. https://doi.org/10.1016/j.carbpol.2018.03.101

[30] J. Desbrieres, C. Martinez, M. Rinaudo. Hydrophobic derivatives of chitosan: characterization and rheological behavior, Int. J. Bio. Macromol. 19 (1996) 21-28. https://doi.org/10.1016/0141-8130(96)01095-1

[31] J. Desbrieres, M. Rinaudo, V. Babak, G. Vikhoreva. Surface activity of water soluble amphiphilic chitin derivatives, Polym Bull. 39 (1997) 209-215. https://doi.org/10.1007/s002890050140

[32] S. Ogawa, E. Decker, D. McClements. Production and Characterization of O/W Emulsions Containing Cationic Droplets Stabilized by Lecithin−Chitosan Membranes, J. Agr. Food Chem. 51 (2003) 2806–2812. https://doi.org/10.1021/jf020590f

[33] A. S. Bellé, C. R. Hackenhaar, L. S. Spolidoro, E. Rodrigues, M. P. Klein, P. F. Hertz. Efficient enzyme-assisted extraction of genipin from genipap (*Genipa americana* L.) and its application as a crosslinker for chitosan gels, Food chem. 246 (2018) 266-274. https://doi.org/10.1016/j.foodchem.2017.11.028

[34] M. K. Shanmugam, H. Shen, F. R. Tang, F. Arfuso, M. Rajesh, L. Wang, A. P. Kumar, J. Bian, B. C. Goh, A. Bishayee, G. Sethi. Potential role of genipin in cancer therapy, Pharmacol. Res. 133 (2018) 195-200. https://doi.org/10.1016/j.phrs.2018.05.007

[35] E. Colombo, F. Cavalieri, M. Ashokkumar. Role of counterions in controlling the properties of ultrasonically generated chitosan-stabilized oil-in-water

emulsions, ACS Appl. Mater. Interfaces. 7 (2015) 12972-12980. https://doi.org/10.1021/acsami.5b02773

[36] K. Kaminski, K. Zazakowny, K. Szczubiałka, M. Nowakowska. pH-sensitive genipin-cross-linked chitosan microspheres for heparin removal. Biomacromol. 9 (2008) 3127-3132. https://doi.org/10.1021/bm800724q

[37] R. Harris, E. Lecumberri, A. Heras. Chitosan-genipin microspheres for the controlled release of drugs: clarithromycin, tramadol and heparin. Mar. drugs, 8 (2010) 1750-1762. https://doi.org/10.3390/md8061750

[38] M. J. Moura, S. P. Martins, B. P. Duarte. Production of chitosan microparticles cross-linked with genipin–Identification of factors influencing size and shape properties. Bioch. Eng. Journal. 104 (2015) 82-90. https://doi.org/10.1016/j.bej.2015.04.017

[39] W. Abdelwahed, G. Degobert, S. Stainmesse, H. Fessi. Freeze-drying of nanoparticles: formulation, process and storage considerations. Adv. Drug Deliv. Rev. 58 (2006) 1688-1713. https://doi.org/10.1016/j.addr.2006.09.017

[40] Adams R P. Identification of essential oil components by gas chromatography/mass spectrometry, 4.1th edition. Allured Publishing Corporation, Illinois; 2017: 809.

[41] D. M. Casa, T. C. M. M. Carraro, L. E. A. Camargo, L. F. Dalmolin, N. M. Khalil, R. M. Mainardes. Poly(L-lactide) Nanoparticles Reduce Amphotericin B Cytotoxicity and Maintain Its In Vitro Antifungal Activity. J. Nanosci Nanotechnol. 15 (2015) 848-854. https://doi.org/10.1166/jnn.2015.9177

[42] S. Sahu, S. Saraf, C. D. Kaur, S. Saraf. Biocompatible nanoparticles for sustained topical delivery of anticancer phytoconstituent quercetin. Pak J Biol Sci. 16 (2013) 601-609. https://scialert.net/abstract/?doi=pjbs.2013.601.609

[43] S. A. Abouelmagd, B. Sun, A. C. Chang, Y. J. Ku, Y. Yeo. Release Kinetics Study of Poorly Water-Soluble Drugs from Nanoparticles: Are We Doing It Right?. Mol. Pharm. 12 (2015) 997-1003. https://doi.org/10.1021/mp500817h

[44] B. Lu, X. Lv, Y. Le. Chitosan-Modified PLGA Nanoparticles for Control-Released Drug Delivery. Polymers. 11 (2019) 304. https://doi.org/10.3390/polym11020304

[45] E. Grela, J. Koz Owska, A. Grabowiecka. Current methodology of MTT assay in bacteria - A review. Acta Histochem. 120 (2018) 303 – 311. https://doi.org/10.1016/j.acthis.2018.03.007

[46] N. Zhang, R. Yao, J. Guo, J. He, G. Meng, F. Wu. Modulation of osteogenic and haemostatic activities by tuning cationicity of genipin-crosslinked chitosan hydrogels. Colloids Surf. B. 166 (2018) 29-36. https://doi.org/10.1016/j.colsurfb.2018.02.056

[47] P. S. Pourshahab, K. Gilani, E. Moazeni, H. Eslahi, M. R. Fazeli, H. Jamalifar. Preparation and characterization of spray dried inhalable powders containing chitosan nanoparticles for pulmonary delivery of isoniazid. J. Microencapsul. 28 (2011) 605–613. https://doi.org/10.3109/02652048.2011.599437

[48] M. A. Pujana, L. Pérez-Álvarez, L. C. C. Iturbe, I. Katime. Biodegradable chitosan nanogels crosslinked with genipin. Carbohydr. 94 (2013) 836–842. https://doi.org/10.1016/j.carbpol.2013.01.082

[49] M. Lopez, M. A. Blazquez. Characterization of the Essential Oils from Commercial Chamomile Flowers and Chamomile Teabags by GC-MS Analysis. I J Pharmacog and Phytoc R., 8 (2016), 1487 – 1491.

[50] L. Ma, C. Shen, L. Gao, D. Li, Y. Shang, K. Yin, D. Zhao,W. Cheng, D. Quan. Anti-inflammatory activity of chitosan nanoparticles carryingNF- B/p65 antisense oligonucleotide in RAW264.7 macrophage stimulated by lipopolysaccharide. Colloid Surface B, 142 (2016), 297–306. 10.1016/j.colsurfb.2016.02.031

[51] L. Q. Jiang, T. Y. Wang, T. J. Webster, H. Duan, J. Y. Qiu, Z. M. Zhao, X. X. Yin, C. L. Zheng. Intracellular disposition of chitosan nanoparticles in macrophages: intracellular uptake, exocytosis, and intercellular transport. Int. J. Nanomedicine. 12 (2017), 6383–6398. 10.2147/IJN.S142060

Supplementary data

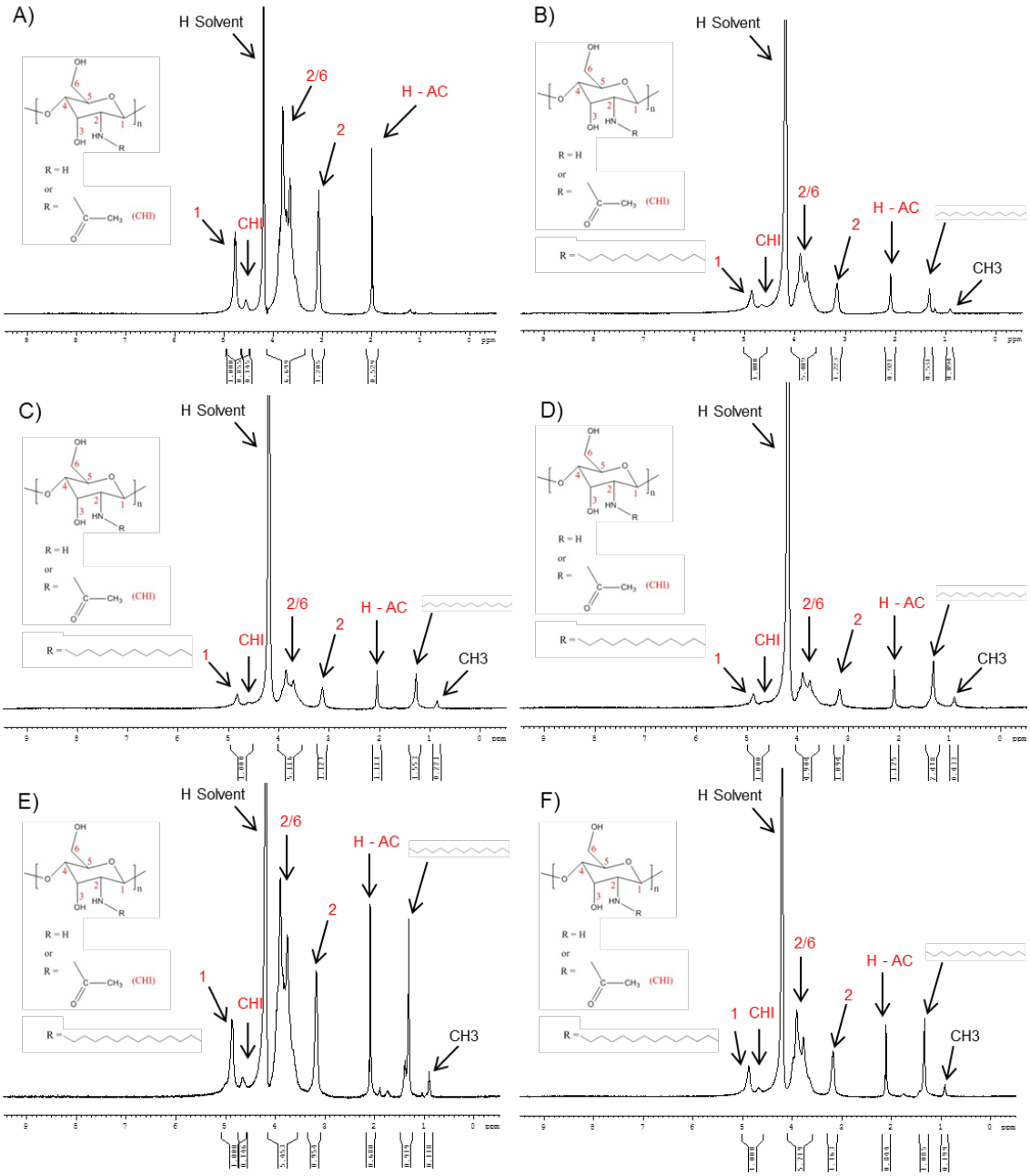

Figure S1. ^{1}H NMR spectrum of the different *N*-alkyl CHI derivatives solubilized in 1% CD_3COOD/D_2O. A) Chitosan Primex; B) CHI_3C_{12}; C) CHI_8C_{12}; D) $CHI_{13}C_{12}$; E) CHI_4C_{14}; E) CHI_6C_{14}.